Pivot Algorithm Computer Simulation of the Effect of Grafted Polymers on the Adsorption of Polymers by a Surface

Thomas C. Clancy and S. E. Webber*

Department of Chemistry and Biochemistry and Center for Polymer Research, University of Texas at Austin, Austin, Texas 78712

Received July 15, 1994; Revised Manuscript Received February 3, 1995[⊗]

ABSTRACT: Monte Carlo simulations are used to calculate monomer distribution profiles and adsorption isotherms of moderately dense end-grafted and adsorbed polymer chains. Modified variants of the pivot algorithm on a cubic lattice are combined with a fixed end points pivot algorithm to allow simulation in regimes where normal pivoting is ineffective due to excluded volume effects. Scaling behavior that agrees with analytical theory for low density and a brush is obtained for the end-grafted case, which illustrates the accuracy of this method applied to polymers that are overlapping. For polymers in the solution phase a Monte Carlo move of the center of mass of the polymer is added to the normal pivot moves. The surface excess is obtained by integrating $\phi(z)-\phi_b$ and can be treated by the Langmuir model to obtain the apparent maximum surface excess (Γ_{exc}^{max}) as a function of the bulk monomer concentration (ϕ_b). It is found that the presence of end-grafted nonadsorbing polymers can affect competitive adsorption of different length chains. In particular, high molecular weight polymers may be preferentially excluded from a polymer-grafted surface, unlike a bare surface.

1. Introduction

The properties of polymers at interfaces are relevant in a variety of contexts including biological, colloidal, chromatography, and surfactant systems. These properties have been studied by various theoretical and experimental techniques. Analytical and numerical theories, particularly scaling and mean field approaches, have been applied toward understanding the structure of polymers in such environments. Experimental work aimed at obtaining detailed structural information in these systems has proven difficult.[1-4] For a recent review, see Kawaguchi and Takahashi.[5] Kawaguchi has also reviewed polymer adsorption.[6]

In an earlier paper we have applied the pivot algorithm[7] to a low density of block polymers, alternating polymers, and homopolymers at liquid–liquid or liquid–solid interfaces.[8] While the pivot method is known to be an excellent algorithm for a low coil density, we are not aware of prior work that has tested this method in the regime in which polymer–polymer interactions are significant. We apply this method to three problems: (1) end-grafted polymers of length N_g at graft densities above and below R_g^{-2}, where R_g is the radius of gyration of the end-grafted polymer; (2) the adsorption of free polymers in solution for bulk volume fractions (ϕ_b) as high as c^* ($=N_b^{-4/5}$, where N_b is the segment length of the polymer in bulk solution); (3) the adsorption of free polymers in solution of length N_b onto a surface with varying densities of end-grafted polymers of length N_g. In the first case we recover the scaling results of Milner et al.[1] as was also demonstrated by Chakrabarti et al.[9] using a standard Monte Carlo approach for zero adsorption energy. Our method could be extended easily to include solvent or surface energetic terms although that is not the point of the present calculations. Although the acceptance fraction for the pivot method decreases as the grafting density increases, it is still quite satisfactory into the brush regime. In the second case we can compute the segment profile for various surface adsorption energies (we treat the solvent as athermal) and use this profile to compute a surface excess (Γ_{exc} in the notation of Scheutjens and Fleer (SF)[10]). We find Γ_{exc} to increase with ϕ_b toward a limiting value. As expected, Γ_{exc} increases with N_b for constant ϕ_b and χ_s (surface adsorption energy in units of kT[11]). The segment profiles have very little statistical variation, indicating the high accuracy of the pivot method in this application.

Finally, we examine bulk polymer adsorption on a surface with end-grafted polymers. While we are aware of recent scaling studies of a problem of this type[12] which builds on the work of de Gennes,[13] we are not aware of any simulation studies of the type presented herein. One of the interesting results we obtain is that one can obtain "size exclusion" by controlling the length of the graft polymer (N_g) with respect to the bulk polymer (N_b). Thus one can offset the tendency of a long polymer to adsorb onto a surface and preferentially adsorb short polymers at constant χ_s. While this steric exclusion is not surprising, the explicit use of a simulation permits one to examine the effect of polymer architecture, adsorption or solvent energetics, and molecular weight to control adsorption. This seems to us to have obvious implications for the rational design of polymer coatings in chromatographic applications.

There are many papers that deal with polymer adsorption at surfaces. Our rationales for presenting the present calculations are the following:

(1) Wang and Mattice[14] have recently compared the SF mean-field method with a multichain Monte Carlo calculation and found systematic errors in the mean-field results, although all qualitative features are reproduced. This is believed to be the result of some of the assumptions that are inherent to mean-field methods. Since the pivot method (with the modifications presented later) is an efficient Monte Carlo method when applied to these problems, we expect many interesting systems can be studied using it. However, it will definitely break down at high polymer densities because of the low acceptance fraction (see later discussion).

(2) Scaling results provide many global insights as to the effect of molecular weight, grafting densities, or polymer structure. However, these scaling results do not permit one to examine the result of modifying the molecular details of the polymer (i.e., balancing the

[⊗] Abstract published in *Advance ACS Abstracts,* March 15, 1995.

0024-9297/95/2228-2561$09.00/0 © 1995 American Chemical Society

effects of a more strongly adsorbing group or sequence distribution against molecular weight). Thus scaling results can help guide Monte Carlo simulation but do not necessarily help the polymer chemist to design a better polymer. It is in the latter area that we believe the present results may be of most use.

2. Background

Polymers at solid–liquid interfaces are expected to be perturbed from their random coil solution conformation by interactions with the surface and with other polymers. Two typical examples are end-grafted nonadsorbing polymers and adsorbed homopolymers. Numerical lattice-based calculations have been used extensively to predict equilibrium properties and chain conformation of adsorbed polymers.[10,15,16] Scaling approaches have also been applied to polymer adsorption.[17] In general, it is expected that monolayer adsorption should cause adsorbed polymer chains to flatten out to form a two-dimensional random coil structure.

In the end-grafted case at densities high enough to cause overlap between the different polymer coils the chains stretch out perpendicularly with respect to the interface, forming a polymer brush.[1,2] Usually, the density of monomers as a function of distance from the surface (monomer distribution profile) and the distribution of distances of the free end from the surface are used to characterize the average conformational structure. The initial scaling approaches assumed a steplike profile with depletion near the interface and with all free ends at the exterior of the brush.[13,18] The analytical self-consistent field result predicts a maximum at the interface with a parabolic decay.[1] Computer simulations have yielded a profile with features predicted by both theories, showing a depletion near the interface, followed by a parabolic decay.[9]

Polymer brushes have been simulated by molecular dynamics with each monomer coupled to a heat bath,[19] by the use of a bond fluctuation model Monte Carlo method,[20,21] by a Monte Carlo dynamics method,[22] and by a Monte Carlo simulation on a lattice.[9] This latter simulation employed local (short range) Monte Carlo moves which change only a small section of the polymer chain (one or two monomers) with each Monte Carlo step. This type of algorithm is known to have extremely long relaxation CPU times[7] due to the large-scale structure of polymer chains. The simulation presented in section 4.1 treats the same problem as Chakrabarti et al.,[9] yielding essentially identical results, but using the pivot algorithm which changes larger sections of the polymer chain with each step.

The original pivot algorithm was developed for isolated isotropic linear chains.[7,23] This algorithm has been modified slightly to study other architectures such as star polymers[24,25] and comb polymers[26] as well linear polymers interacting with one[8] or more[27] interfaces. Previously, we have simulated polymers and copolymers adsorbed at liquid–liquid and solid–liquid interfaces in the dilute limit.[8] In the results presented herein, the effect of finite concentration is simulated, demonstrating the effects of multiple chain interaction on such quantities as surface adsorption saturation. Because of this high segment density it is necessary to add another type of pivoting move. It consists primarily of the combination of a modified pivot algorithm[8] with a fixed-point pivot-type algorithm[28] to move internal sections of the chain. This allows the use of a pivot algorithm in moderately concentrated ($\phi_b = 0.4$) regimes. Some of the common dynamic Monte Carlo cubic lattice chain moves such as crankshaft rotations, end turns, and bend flips (but not reptation) are a subset of the movements of this generalized pivot algorithm. Although not used here, the analogous reptation move would be one in which the chain reptates in random directions by more than one unit (randomly selected from 1 to N) along the lattice. The acceptance fraction would be expected to decrease, while the difference between the new and old chain would be greater as with the pivot algorithm. However, as far as we know, no detailed analysis of such an algorithm has been undertaken as with the pivot algorithm.

3. Simulation Details

The pivot algorithm is a dynamical Monte Carlo algorithm which generates new chain conformations from previous conformations by the use of a Monte Carlo pivoting move.[7,23] For computational convenience the conformations are usually constrained to lie on a lattice, but this is not a requirement. The polymer chain is modeled as N monomer units contiguously linked as a self-avoiding walk on the lattice. The Monte Carlo move consists of the random selection of a monomer, j ($1 < j < N$), along the chain which bisects this chain into two sections. A symmetry operation is randomly selected from the appropriate point group (O_h for a simple cubic lattice) and one section of the chain is moved according to the selected symmetry operation. If the new conformation obeys the excluded volume constraint, the pivot move is allowed. If not, a move is attempted again with another randomly selected pivot point and symmetry operation.

To simulate relatively short isolated athermal end-grafted chains at an impenetrable interface, all that is necessary is to begin with a conformation which has one end at the surface and to consistently pivot the section of the bisected chain which is not attached to the interface with respect to the other section. If the new conformation obeys the excluded volume and surface impenetrability constraints, the pivot move is allowed and a new conformation has been generated. In order to simulate multiple interacting end-grafted chains at finite grafting density, σ, a second type of pivoting move was added. Two pivot points on the chain (j, k; $k > j + 1$) are randomly selected. This divides the chain into three sections, the middle section of which is pivoted. The Monte Carlo move here is essentially the pivot algorithm for fixed end points as invented by Madras et al.[28] and applied only to this middle section. A symmetry operation is chosen which will change the coordinates of the middle section while leaving the positions of the two pivot points fixed. The types of symmetry operations allowed will depend on the relative geometric position on the lattice of the two randomly selected pivot points. If the two points are collinear or coaxial with respect to the lattice, a larger number of symmetry operations are available. In general, only inversion with respect to the geometric center of the two pivot points, followed by order reversal of the m pivoted monomers ($j \le m \le k$) will be an acceptable symmetry operation. This second type of pivoting move (internal pivoting) is necessary in order to simulate polymer chains in denser environments. Figure 1 shows a representative internal pivoting move in two dimensions. Monomers 3–10 are pivoted (using the symmetry operation C_2 or i), followed by reverse renumbering of these monomers. A Monte Carlo move was allowed only

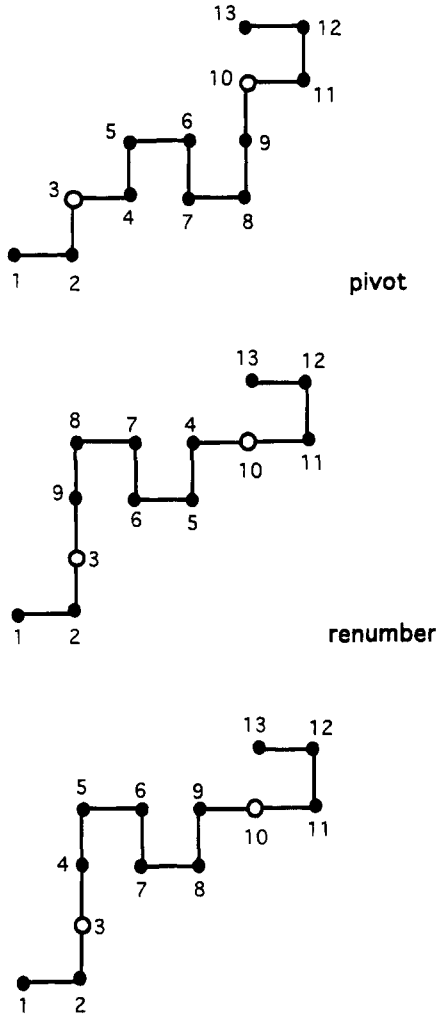

Figure 1. Illustration of internal pivoting.

if the new conformation did not penetrate the interfacial plane and if it obeyed the excluded volume constraint with respect to the same chain or other chains.

To simulate adsorbed and bulk solution polymer chains, a pivot point, j, was randomly chosen, and then it was randomly decided whether to pivot the first section of the chain (monomers, m: $m < j$), the second section ($m > j$), or the whole chain. Translation of the entire chain by one or more lattice units was an additional Monte Carlo move. To simulate multiple surface grafted chains, the internal pivoting move with fixed end points was added since higher densities may cause the chains to be geometrically constrained by excluded volume effects. In all cases, the Monte Carlo move was allowed only if the new conformation obeyed the excluded volume and surface impenetrability constraints. The surface adsorption energy is then calculated (see below).

The solid–liquid interface is defined as a rectangular box with a square face in the x–y plane having an impenetrable surface located at $z = 0$ in the lattice coordinate space. End-grafted chain ends are randomly placed on the face at $z = 0$. Bulk polymer chains are allowed to move anywhere, within the constraints of excluded volume and surface impenetrability. Periodic boundary conditions are applied in the x and y directions.

No energetic parameters are employed with respect to the end-grafted polymers other than excluded volume. For the bulk polymers a short-range attractive monomer–surface interaction energy, χ_s, given in units of kT is included along with the excluded volume constraint. The energy, E, of the system is the sum of all monomers of the adsorbing polymers in contact with the surface, c_w (monomers with coordinate $z = 0$) multiplied by χ_s as given by eq 1.

$$E = -c_w\chi_s \tag{1}$$

Metropolis importance sampling is applied with respect to each Monte Carlo step.[29] The chains are allowed to thermalize for a large number of pivot moves before the chain conformations are sampled.

4. Results and Discussion

4.1. End-Grafted Polymers. The Low-Density ("Mushroom") Regime. At low grafting density ($\sigma \cong 1/N_g$), the coils perturb each other only slightly and stretching of the chains is weak. The monomer ($\phi(z)$) and end-monomer ($e(z)$) profiles scale approximately as isolated coils.[18]

$$\frac{\phi(z)}{\sigma(N_g - 1)^{2/5}} \sim \frac{z}{(N_g - 1)^{3/5}} \tag{2}$$

$$\frac{e(z)}{\sigma(N_g - 1)^{2/5}} \sim \frac{z}{(N_g - 1)^{3/5}} \tag{3}$$

In Figure 2 we plot the $\phi(z)$ (Figure 2a) and $e(z)$ (Figure 2b) results from our simulation scaled according to eqs 2 and 3. The agreement is very good. A scaled profile from an ensemble with higher grafting density ($N_g = 50$, $\sigma = 0.056$) is also shown to illustrate the difference in the scaling behavior (see next subsection).

The High-Density ("Brush") Regime. At higher grafting density the coils overlap significantly and the results of Milner et al.[1] suggest a scaling relationship as given by eqs 4 and 5.

$$\frac{\phi(z)}{\sigma^{2/3}} \sim \frac{z}{(N_g - 1)\sigma^{1/3}} \tag{4}$$

$$\frac{e(z)(N_g - 1)}{\sigma^{2/3}} \sim \frac{z}{(N_g - 1)\sigma^{1/3}} \tag{5}$$

Figure 3 shows the monomer and end distribution results scaled according to eqs 4 and 5. The results are in agreement with ref 9. For comparison, an ensemble with lower grafting density ($N_g = 50$, $\sigma = 0.02$) is also shown.

Although a direct comparison of computational efficiency is difficult, it is expected that an algorithm employing nonlocal (global) moves would be much more efficient than one employing only local moves. This is particularly true in the initial step of thermalization, especially for very long chains[7,28] and for lower grafting densities where chain stretching is minimal, though present. As expected, the acceptance fraction (f_g) decreases rapidly with σ (see Table 1).

Our numerical results suggest that the transition from isolated, tethered chains ("mushrooms") to a stretched brush occurs over the grafting density range $\sigma < R_g^{-2}$ to $\sigma > R_g^{-2}$, respectively (R_g is the radius of gyration of the grafted chain at low density). This is in agreement with scaling analysis.[12] We compare the low- and high-density σ values we use with R_g^{-2} for isolated

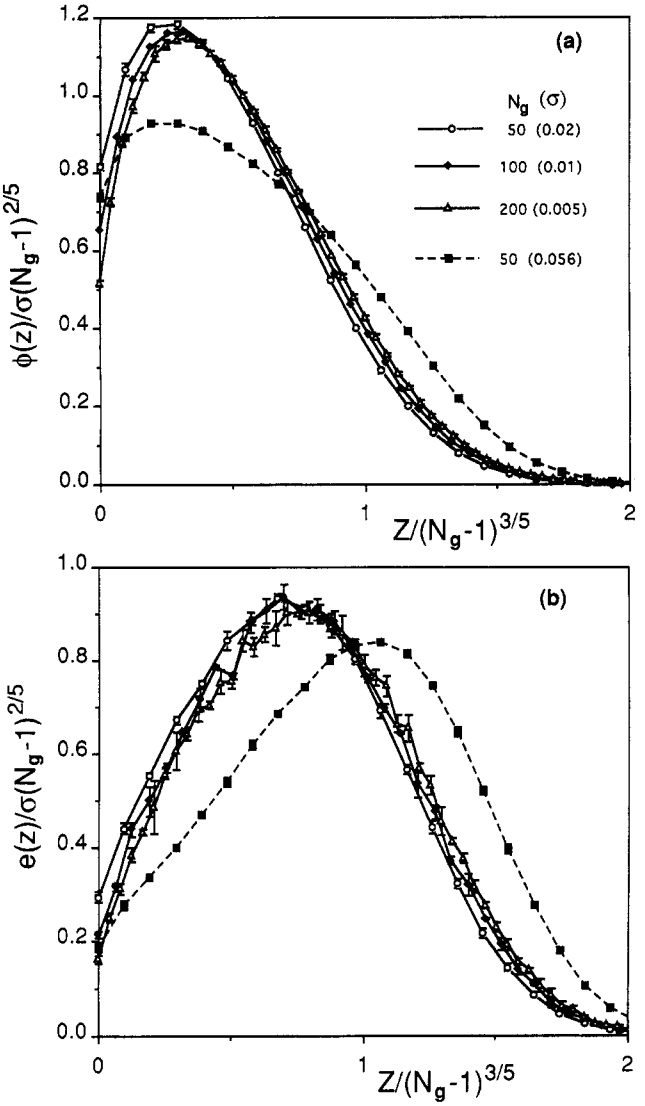

Figure 2. (a) Monomer distribution profiles, $\phi(z)$, and (b) end distribution profiles, $e(z)$, scaled according to eqs 2 and 3 (see text). An ensemble at higher grafting density is also shown for comparison.

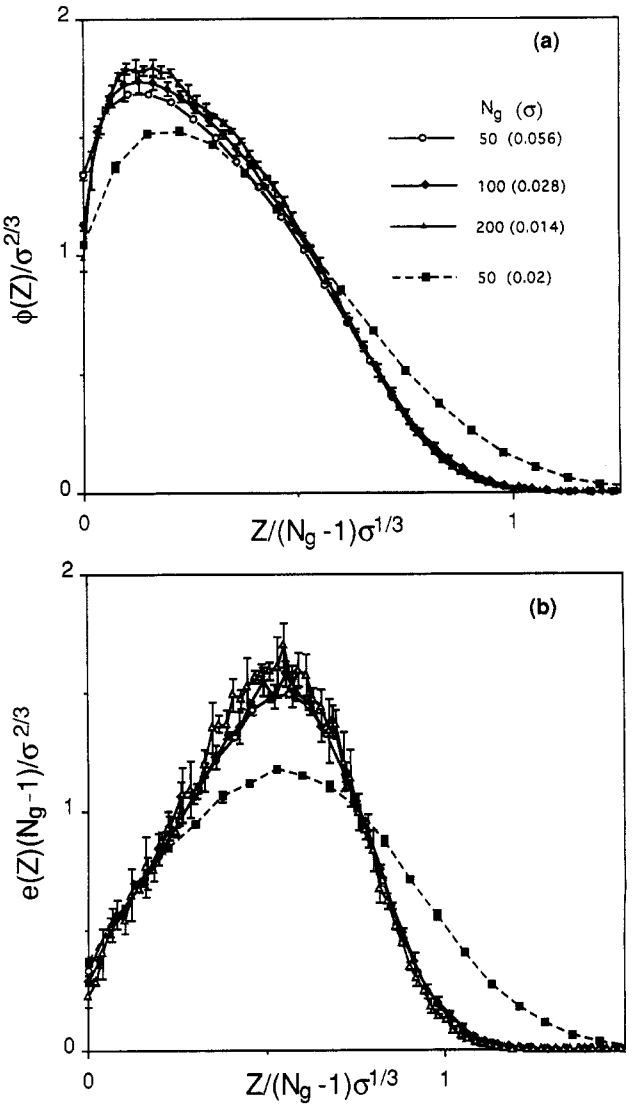

Figure 3. (a) Monomer distribution profiles, $\phi(z)$, and (b) end distribution profiles, $e(z)$, scaled according to eqs 4 and 5 (see text). An ensemble at lower grafting density is also shown for comparison.

end-grafted chains in Table 2. One can compute the components of R_g^2 which are perpendicular and parallel to the surface ($R_g^2 = (R_g^2)_\perp + (R_g^2)_\parallel$). If these are plotted as a function of $\sigma N_g^{6/5}$, we observe that $(R_g^2)_\perp = (R_g^2)_\parallel$ at approximately the same $\sigma N_g^{6/5}$ value (3.4 ± 0.15) for a number of different values of N_g. For densities above and below this point the $\phi(z)$ and $e(z)$ profiles scale like a brush and mushroom, respectively. While we certainly do not have an adequate number of data points to quantitatively analyze this result, it is consistent with the major axis of the R_g^2 ellipsoid being oriented perpendicular to the surface with a numberical value of ca. twice the minor components which are parallel to the surface. For a self-avoiding athermal random walk chain in isotropic solution the ratio of the major component of R_g^2 to the sum of the minor components is ca. 3.24[30] and for end-tethered chains at low density with $\chi_s = 0$ we find the $(R_g^2)_\perp$ to $(R_g^2)_\parallel$ ratio to be ca. 0.6. Hence it seems likely that brush formation occurs when the surface density of polymers begins to force the major axis of the polymer coil to be oriented perpendicular to the surface.

Obviously these simulations could be extended to study this transition as a function of polymer architecture and energetics but that is not the purpose of the present paper. Our goal in this section is to demonstrate that the pivot method can be applied effectively to grafting densities that produce brush morphologies.

4.2. Chains Adsorbed from Solution. Figure 4 shows the monomer distribution profiles for chains at two different equilibrated bulk monomer concentrations, ϕ_b with $\chi_s = +0.5$ on a bare surface. The initial bulk concentration (ϕ_b^0) is shown for comparison. The surface excess, Γ_{exc}, was calculated by summing the increased concentration near the surface (see eq 6). The surface coverage (θ) is obtained by simply counting the number of polymer segments that contact the surface divided by the number of surface lattice sites. In Figure 5a are plots of Γ_{exc} and θ versus ϕ_b for various chain lengths and concentrations, with $\chi_s = +0.5$. The longer chains are preferentially adsorbed, as expected.

There are several different ways to characterize polymer adsorption. Equation 6 corresponds to Γ_2 used by Roe[31] (his equation (32)) and Γ_{exc} defined by Scheutjens and Fleer (SF)[10] (their equation (47)). SF also define a quantity Γ, which is the difference of ϕ_i and the profile of bulk polymers that have no contacts with the surface; i.e., compare

Table 1. Acceptance Fractions for End-Grafted and Bulk Polymer Chains (f_g and f_b) as a Function of Grafting Density (σ), Bulk Solution Average Concentration (ϕ_b), and End-Grafted and Bulk Chain Lengths (N_g and N_b, Respectively)[a]

σ	ϕ_b ($\times 10^4$)	Γ_{exc}	N_g	N_b	f_g	f_b	no. of pivots ($\times 10^{-3}$)	CPU time (s)
0.02			50		0.340		255	1895[b]
0.056			50		0.214		1060	8204[b]
0.125			50		0.130		648	7007[b]
0.01			100		0.277		135	1392[b]
0.028			100		0.093		88.3	1920[b]
0.005			200		0.173		164	4640[b]
0.014			200		0.060		57.2	2326[b]
	91.0	0.56	*d*	100		0.305	275	2780[c]
	168.3	0.59	*d*	100		0.308	258	3891[c]
	266.9	0.57	*d*	100		0.301	234	5193[c]
0.05	86.2	0.32	10	100	0.551	0.231	356	1473[c]
0.01	19.7	0.45	50	100	0.416	0.154		
0.02	375.4	0.291	50	100	0.337	0.319		

[a] All values (except f_g and f_b) are in lattice units. [b] Cray YMP. [c] IBM RISC/6000. [d] For adsorption onto a bare surface.

Table 2. Comparison of σ Values to R_g^{-2}

N_g	σ^b	σ^c	R_g^{-2} [a]
50	0.02	0.056	0.0491
100	0.01	0.028	0.0211
200	0.005	0.014	0.0090

[a] For end-grafted chains at low density. [b] At this grafting density the polymers is in the "mushroom" regime (see section 4.1). [c] At this grafting density the polymer is in the "brush" regime (see section 4.1).

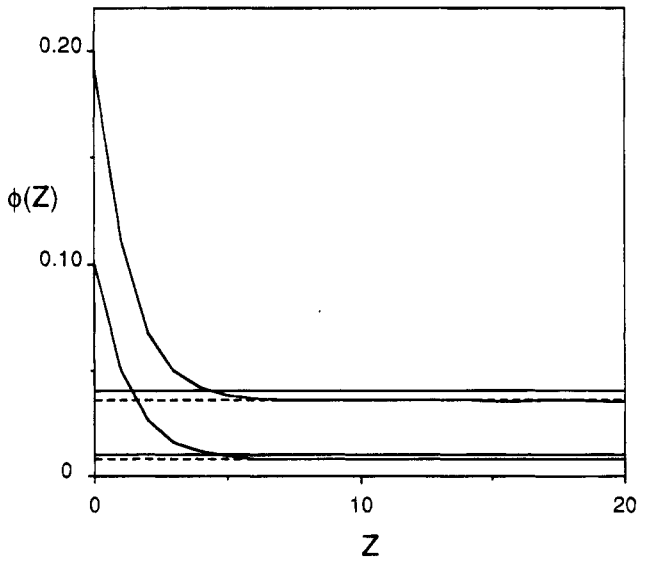

Figure 4. Monomer distribution profiles, $\phi(z)$, for adsorbed chains with different equilibrium bulk monomer concentrations, ϕ_b. The straight solid line is the value of the monomer concentration before adsorption ($\phi_b^0 = 0.011$ and 0.041 for the lower and upper curves, respectively) Γ_{exc} is the area above the dashed line ($\phi_b = 0.008$ and 0.036, respectively). ($N_b = 25$ and $\chi_s = +0.5$).

$$\Gamma_{exc} = \sum_{i=1}^{M} (\phi_i - \phi_b) \tag{6}$$

$$\Gamma = \sum_{i=1}^{M} (\phi_i - \phi_i^f) = \langle n_s \rangle N_b / L_x L_y \tag{7}$$

where ϕ_i is the segment density in the ith layer, ϕ_b is the asymptotic bulk density of segments, and ϕ_i^f is the density of segments of chains that have no contact with the surface (M is the total number of layers). As one moves away from the surface ϕ_i^f must approach ϕ_b. The second form in eq 7 was used by Wang and Mattice[14] to compute Γ. In eq 7 $\langle n_s \rangle$ is the average number of chains in contact with the surface and $L_x L_y$ is the area of the absorbing surface. Note that $\Gamma > \Gamma_{exc}$ with this definition because of surface depletion (see Figure 2 of ref 10). Γ and Γ_{exc} should be very similar numerically for low values of ϕ_b since the surface depletion of free polymers is so small. Since the volume fraction cannot exceed unity, one expects Γ_{exc} to reach a maximum or minimum value as ϕ_b is increased and then approach zero[32] while Γ will reach a plateau. We note that Γ_{exc} is the experimental quantity that is directly measured by many techniques,[33] and it is this quantity that we believe is most relevant to polymer fractionation, as is discussed in the next paragraph and section 4.3. Thus we emphasize Γ_{exc} in our discussions that follow.

Γ_{exc} is directly related to the measurement of the adsorbed amount of polymer by depletion methods. If a polymer solution has an initial volume fraction ϕ_b^0, then after equilibration the bulk concentration will be decreased to ϕ_b (see Figure 4). By conservation of mass the change is related to Γ_{exc}; i.e.

$$\Gamma_{exc} = (\phi_b^0 - \phi_b)L \tag{8}$$

The amount of polymer adsorbed for a given volume to surface area ratio is given by[34]

$$A_{ad} = \Delta\phi_b(V/S) = \Gamma_{exc} \tag{9}$$

where from eq 8 $\Delta\phi_b = \phi_b^0 - \phi_b = \Gamma_{exc}/L$ and for a box with sides of length L, $V/S = L$. Thus Γ_{exc} as a function ϕ_b is directly related to the experimental isotherm. In most experimental cases ϕ_b^0 is sufficiently close to ϕ_b because of the large V/S ratio that the adsorption isotherm can be derived from either ϕ_b or ϕ_b^0. For our small V/S ratios there can be a significant difference between ϕ_b and ϕ_b^0 when ϕ_b^0 is small. In all cases we use the equilibrated final concentration ϕ_b as our adsorption isotherm variable.

The plots of Γ_{exc} or θ vs ϕ_b in Figure 5a have the appearance of a Langmuir isotherm (which is commonly observed experimentally), even for $\phi_b > c^* = N_b^{-4/5}$ in the case of $N_b = 50$ and 100 (c^* for $N_b = 25$ is ca. 0.076, which is slightly above the range of ϕ_b calculated). We find it useful to extract the apparent maximum surface excess (Γ_{exc}^{max}) or maximum surface coverage (θ^{max}) by plotting the data in the linearized form of the Langmuir isotherm:[35]

$$\phi_b/\Gamma_{exc} = \phi_b/\Gamma_{exc}^{max} + 1/(K\Gamma_{exc}^{max}) \tag{10a}$$

$$\phi_b/\theta = \phi_b/\theta^{max} + 1/(K'\theta^{max}) \tag{10b}$$

Γ_{exc}^{max} or θ^{max} are the surface excess of surface coverage maximum at this value of χ_s, and K and K' are

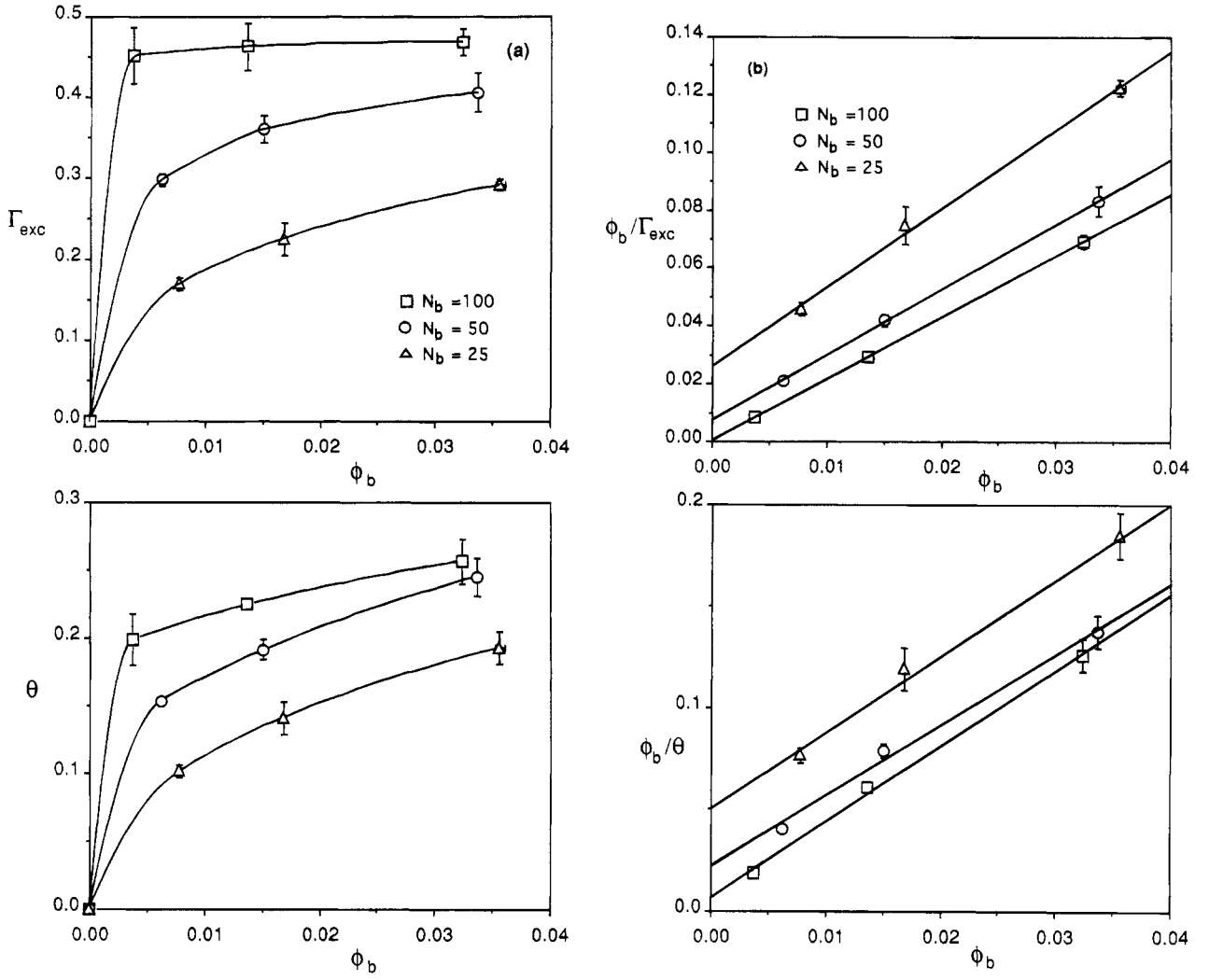

Figure 5. (a) Plot of the monomer surface excess, Γ_{exc}, and surface coverage, θ, versus bulk solution monomer concentration, ϕ_b, for adsorbing chains with $N_b = 25$, 50, 100 and absorption strength $\chi_s = +0.5$. (b) Plot of ϕ_b/Γ_{exc} and ϕ_b/θ versus ϕ_b according to eq 10 for the same ensembles. In this and subsequent plots standard deviations for all parameters were calculated but the error bars were frequently smaller than the plotting symbols.

Table 3. Γ_{exc}^{max} and θ^{max} (±Standard Deviation) as a Function of N_b and χ_s[a]

	χ_s					
	0.5		0.75		1.00	
N_b	Γ_{exc}^{max}	θ^{max}	Γ_{exc}^{max}	θ^{max}	Γ_{exc}^{max}	θ^{max}
25	0.37 ± 0.02	0.26 ± 0.02	0.602 ± 0.004	0.43 ± 0.01	0.81 ± 0.03	0.595 ± 0.009
50	0.443 ± 0.008	0.29 ± 0.02	0.69 ± 0.02	0.462 ± 0.003	0.93 ± 0.04	0.584 ± 0.007
100	0.471 ± 0.001	0.27 ± 0.01	0.73 ± 0.02	0.460 ± 0.0005	1.01 ± 0.07	0.60 ± 0.02

[a] Derived from eq 10.

appropriate equilibrium constants for adsorption. Figure 5b plots the data for the same ensembles shown in Figure 5a using eq 10. The intercept is subject to error because it is generally very small and it requires an accurate estimate of the curvature in the Langmuir isotherm. We emphasize that we use eq 10 empirically to obtain the maximum surface excess or coverage. At higher ϕ_b one expects positive deviations from linearity based on the general behavior of Γ_{exc}.[36] In Table 3 we collect Γ_{exc}^{max} and θ^{max} for different values of χ_s and N_b. Γ_{exc}^{max} and θ^{max} increase with increasing χ_s and the higher molecular weight polymers adsorb more strongly, as expected. Note that the different in Γ_{exc}^{max} for the three N_b values for different χ_s remains approximately constant such that changing the surface affinity for the polymer does not provide for size differentiation.

4.3. Chains Adsorbing onto Surfaces with End-Grafted Polymers. The effect of a nonadsorbing end-grafted polymer on the adsorption properties discussed in the previous subsection is considered in this subsection. The simulation is run as described in section 4.2 except that the end-grafted polymer is present. For the bulk polymer in all of these simulations, $\chi_s = +1.0$, with σ for the end-grafted polymer in the weakly overlapping or mushroom regime. Figure 6 shows the monomer distribution profiles for a simulation in which the end-grafted chains are of length $N_g = 50$ and $\sigma = 0.02$ and the bulk solution chains are of length $N_b = 25$ with a bulk monomer concentration $\phi_b = 0.0347$. A depletion zone is created in the free monomer distribution profile by the presence of the end-grafted chains. In a recent paper by Aubouy and Raphäel, scaling arguments were

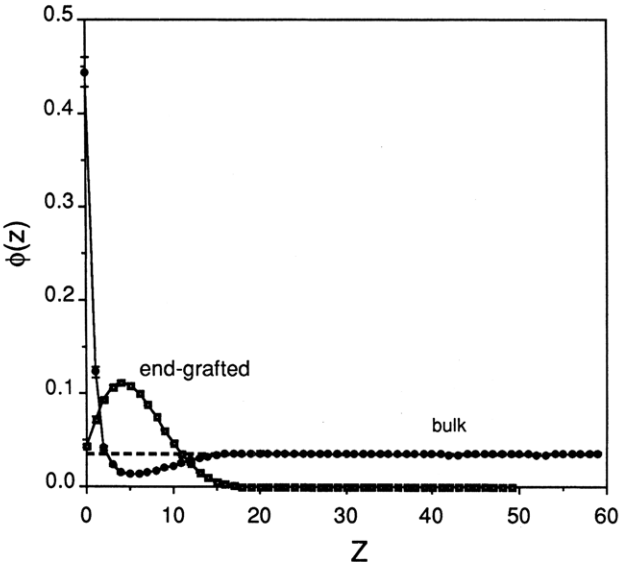

Figure 6. Monomer distribution profiles of end-grafted and bulk polymers ($\chi_s = +1.0$, $\sigma = 0.02$, $\phi_b = 0.0347$, $N_g = 50$, $N_b = 25$).

Scheme 1

R_g = radius of gyration of grafted chain

R_b = radius of gyration of bulk chain

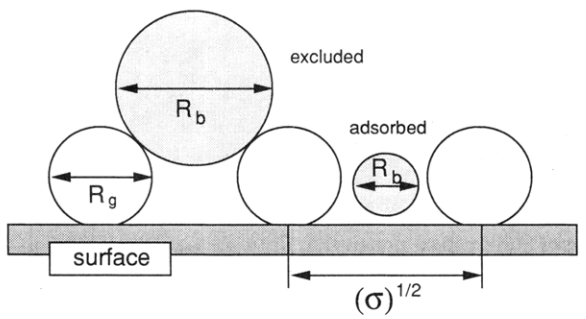

used to analyze the volume fraction profiles of free chains of length P ($\equiv N_b$) in the presence of a surface with end-grafted chains of length N ($\equiv N_g$).[12] While the interaction energy of both chain types with the surface was taken to be zero, the analysis concludes that at low grafting densities, such as the present calculations, one remains in the "mushroom regime" (Figure 1). However, R_g does depend on ϕ_b for $\phi_b > N_b^{-4/5}$, which is near the upper limit of ϕ_b considered in the calculations presented here.[37] While these authors do not consider adsorption isotherms explicitly, they do point out that as the surface forms a brush total exclusion of the free chains should result. Thus the differential size exclusion discussed next would be expected to vanish for $\sigma > R_g^{-2}$, where R_g is the radius of gyration of grafted chains (see section 4.1).

As in the previous subsection, eq 10 is used to obtain Γ_{exc}^{max} and θ^{max} (in this case only the contribution from untethered chains is counted). Parts a and b of Figure 7 show these quantities as a function of σ for bulk polymers of different length ($N_b = 25$, 50, 100) and with the length of the end-grafted chain ($N_g = 50$ and 10, respectively). Γ_{exc}^{max} and θ^{max} decrease systematically with σ as would be expected from steric effects. For higher σ and higher N_g the longer bulk solution chains are preferentially excluded, as shown in Figure 7a. The situation for $N_g = 25$ lies between these extremes and is not shown for brevity (see Table 3 for a comparison of the Γ_{exc}^{max} values). This effect is illustrated in Figure 8 in which Γ_{exc} is plotted $N_b = 100$ and 25 for $\chi_s = 1.0$ as a function of ϕ_b for a bare surface (cf. Figure 5 for $\chi_s = 0.5$[38]) and for a surface with $\sigma = 0.02$ of end-grafted polymer with $N_g = 50$. For the bare surface there is a clear difference in Γ_{exc}, with the longer chain being more strongly adsorbed, as expected. This situation is reversed for the surface with the end-grafted polymer, with $\Gamma_{exc}(N_b=25)/\Gamma_{exc}(N_b=100)$ on the order of 1.7 for $\phi_b > 0.01$. This same ratio for the bare surface is on the order of 0.81. As a further check on this conclusion, simulations were performed for a mixture of $N_b = 10$ and 100 polymers with $\phi_b^0 = 0.015$ for both. After equilibration with a surface with end-grafted chains ($N_g = 50$) at a grafting density of $\sigma = 0.015$, the surface excess of the short chains was ca. 4.6 ($\pm$0.6) times higher than the long chains. On a surface with short end-grafted polymers ($N_g = 10$) at low density ($\sigma = 0.004$) this ratio was ca. 0.64 ($\pm$0.12). Note that this coequilibration reflects not only the different in Γ_{exc}^{max} values but also the "equilibrium constant" K in eq 10a. Thus this method of simulation can easily represent size exclusion at a modified surface.

These results are easy to understand qualitatively. Since the grafted chains are athermal with respect to the free chains, the average attraction of the surface for the free chains diminishes with increasing σ. Larger end-grafted chains provide more efficient steric hindrance per grafting site. When the average spacing between the excluded volume of the end-grafted chains is large compared to the size of the free chain, the surface should behave as a simple surface with diminished χ_s. As stated earlier, for an athermal brush (at high σ) no adsorption is expected and a surface depletion would be observed (we do not go to sufficiently high σ to achieve a brush in the calculations discussed in this subsection). When the size of the bulk polymer (N_b) is on the order of the end-grafted polymer (N_g) at a grafting density on the order of R_g^{-2}, it is necessary to distort both polymers in order for adsorption to occur. Therefore size exclusion for $N_b > N_g$ is expected (Scheme 1). Obviously, the relation between N_g, N_b, σ, and χ_s plus the possible role of solvent–polymer energetics and the size exclusion evidenced in Figure 7 or 8 is complex.

Our goal in these calculations is straightforward: using the present methodology one could estimate the effect of different copolymer compositions and architectures (block, alternating, random) and functional groups (which would affect χ_s) in order to guide the synthesis of surface-modifying polymers for chromatographic applications. Alternatively, these methods could be used to test analytical theory for polymers in the weakly overlapping regime. We would not expect the pivot algorithm as applied in this paper to be adequate for simulations at much higher grafting densities or solution volume fraction than presented herein.

5. Summary

The results obtained with the modified pivot method are generally in accord with the end-grafted Monte Carlo simulation results which uses end turn, bead jump, and crankshaft motion Monte Carlo moves.[9] The "strongly stretched" regime occurs for $\sigma > R_g^{-2}$ but we have not attempted to analyze completely the transition from mushroom to brush in these calculations.

The adsorption of bulk polymers onto a surface could also be simulated effectively. The Langmuir isotherm

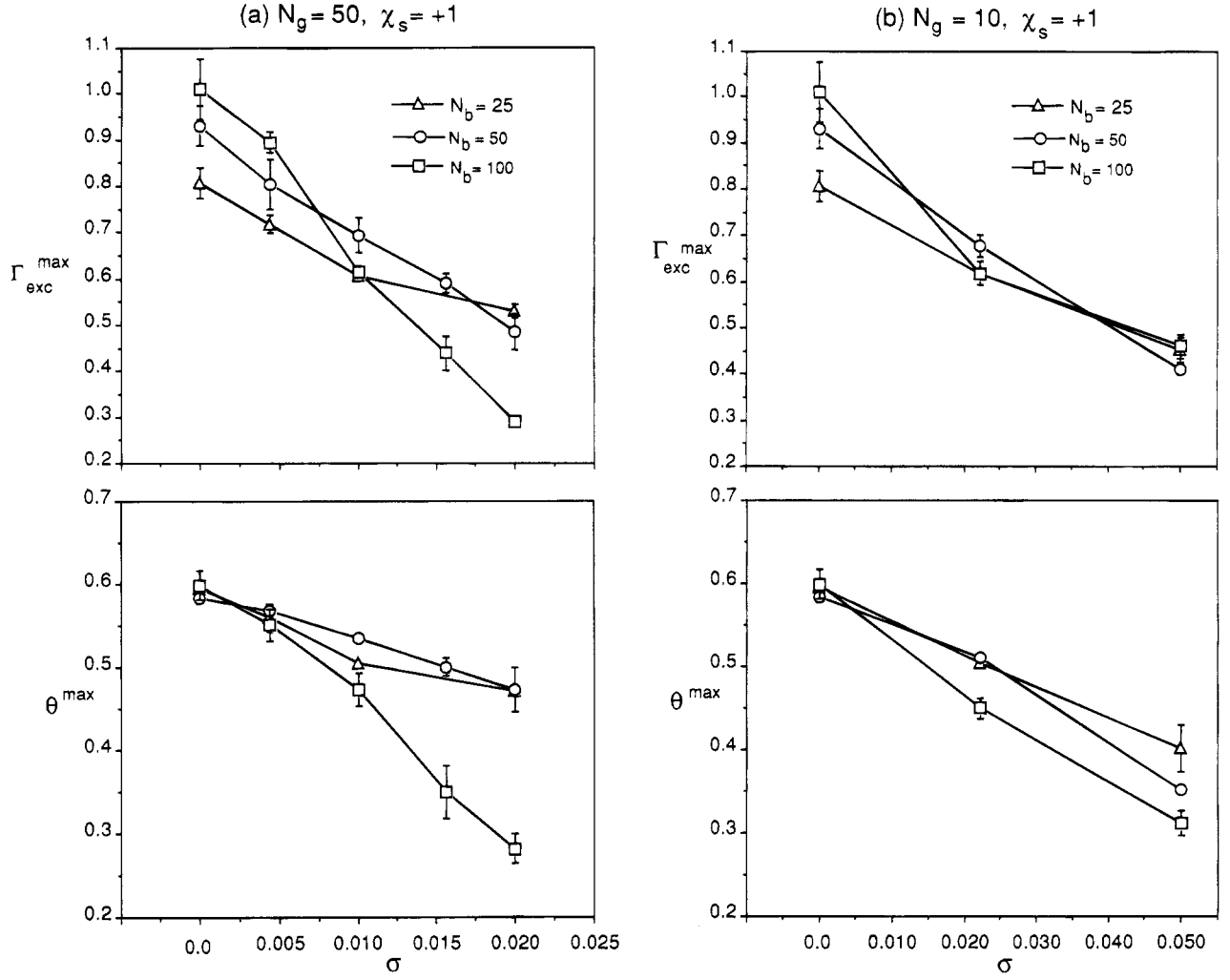

Figure 7. Plots of maximum adsorption, Γ_{exc}^{max} and θ^{max}, as a function of end-grafted density, σ, for $N_b = 25$, 50, 100 and (a) $N_g = 50$ and (b) $N_g = 10$.

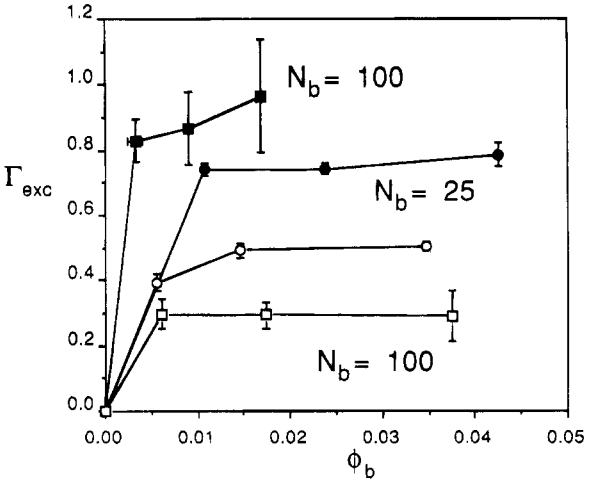

Figure 8. Γ_{exc} versus ϕ_b for $\chi_s = +1.0$ for N_b 25, 100 for a bare surface (upper curves) and a surface with a density of end-grafted polymers $\sigma = 0.02$ with $N_g = 50$ (lower curves). (The error bars for ϕ_b are too small to be seen in most cases.)

for Γ_{exc} (eq 10) was used to estimate the maximum surface excess, Γ_{exc}^{max}, and surface coverage, θ^{max}. Adsorption of bulk polymers at a surface which has variable densities of end-grafted polymers was also simulated. It was found that the presence of end-grafted chains could affect the relative amount of adsorption of different molecular weight polymers, in contrast to a bare surface for which there is always greater adsorption of the higher molecular weight polymers. We are not aware of simulations that predict this effect, which has obvious implications for polymer chromatography.

Acknowledgment. This research has been supported by the National Science Foundation Polymers Program (Grant DMR-9308307) and the Robert A. Welch Foundation (Grant F-356).

References and Notes

(1) Milner, S. T. *Science* **1991**, *251*, 905 and references contained therein.
(2) Halperin, A.; Tirrell, M.; Lodge, T. P. *Adv. Polym. Sci.* **1991**, *100*, 31 and references contained therein.
(3) Takahashi, A.; Kawaguchi, M. *Adv. Polym. Sci.* **1982**, *46*, 1 and references contained therein.
(4) Piirma, I. *Polymeric Surfactants*; Marcel Dekker, Inc.: New York, 1992 and references contained therein.
(5) Kawaguchi, M.; Takahishi, A. *Adv. Colloid Interface Sci.* **1992**, *37*, 219.
(6) Kawaguchi, M. *Ads. Colloid Interface Sci.* **1990**, *32*, 1.
(7) Madras, N.; Sokal, A. D. *J. Stat. Phys.* **1988**, *50*, 109.
(8) Clancy, T. C.; Webber, S. E. *Macromolecules* **1993**, *26*, 628.
(9) Chakrabarti, A.; Toral, R. *Macromolecules* **1990**, *23*, 2016.
(10) (a) Scheutjens, J. M. H. M.; Fleer, J. *J. Phys. Chem.* **1979**, *83*, 1619. (b) Scheutjens, J. M. H. M.; Fleer, J. *J. Phys. Chem.* **1980**, *84*, 178.
(11) In our previous simulations (ref 8) we referred to this quantity as $-\lambda$. We use the symbol χ_s here to conform to earlier work in this field.

(12) Aubouy, M.; Raphaël, E. *Macromolecules* **1994**, *27*, 5182.
(13) de Gennes, P.-G. *Macromolecules* **1980**, *13*, 1069.
(14) Wang, Y.; Mattice, W. L. *Langmuir* **1994**, *10*, 2281.
(15) Levine, S.; Thomlinson, M. M.; Robinson, K. *Discuss. Faraday Soc.* **1978**, *65*, 202.
(16) DiMarzio, E. A.; Rubin, R. J. *J. Chem. Phys.* **1971**, *55*, 4318.
(17) de Gennes, P.-G. *Macromolecules* **1981**, *14*, 1637.
(18) Alexander, S. *J. Phys. (Paris)* **1977**, *38*, 983.
(19) Murat, M.; Grest, G. S. *Macromolecules* **1989**, *22*, 4054.
(20) Lai, P. Y.; Binder, K. *J. Chem. Phys.* **1991**, *95*, 9288.
(21) Dickman, R.; Hong, D. C. *J. Chem. Phys.* **1991**, *95*, 4650.
(22) Milik, M.; Kolinski, A.; Skolnick, J. *J. Chem. Phys.* **1990**, *93*, 4440.
(23) Lal, M. *Mol. Phys.* **1969**, *17*, 57.
(24) Bishop, M.; Clarke, J. H. R. *J. Chem. Phys.* **1991**, *94*, 4009.
(25) (a) Zifferer, G. *Makromol. Chem.* **1990**, *191*, 2717. (b) Zifferer, G. *Makromol. Chem., Theory Simul.* **1992**, *1*, 55.
(26) Gersappe, D.; Harm, P. K.; Irvine, D.; Balazs, A. C. *Macromolecules* **1994**, *27*, 720.
(27) Gersappe, D.; Li, W.; Balazs, A. C. *J. Chem. Phys.* **1993**, *99*, 7209.
(28) Madras, N.; Orlitsky, A.; Shepp, L. A. *J. Stat. Phys.* **1990**, *58*, 159.
(29) Metropolis, N.; Rosenbluth, A. W.; Rosenbluth, M. N.; Teller, A. H.; Teller, E. *J. Chem. Phys.* **1953**, *21*, 1087.
(30) (a) Zifferer, G.; Olaj, O. F. *J. Chem. Phys.* **1994**, *100*, 636. (b) Bruns, W. In *Monte Carlo in Applications in Polymer Science*; Berthierr, G., Ed.; Lecture Notes in Chemistry, Vol. 27; Springer-Verlag: New York, 1991; Chapter 3.
(31) Roe, R.-J. *J. Chem. Phys.* **1974**, *60*, 4192.
(32) This behavior is clearly demonstrated in the calculations of refs 31 and 10.
(33) (a) Stromberg, R. R.; Tutas, D. J.; Passaglia, E. *J. Phys. Chem.* **1965**, *69*, 3955. (b) Kim, M.-W.; Fetters, L. J. *Macromolecules* **1991**, *24*, 4216. (c) Dai, K. H.; Washiyama, J.; Kramer, E. J. *Macromolecules* **1994**, *27*, 4544.
(34) Cohen Stuart, M. A.; Scheutjens, J. M. H. M.; Fleer, G. J. *J. Polym. Sci., Polym. Phys. Ed.* **1980**, *18*, 559.
(35) Attwood, D.; Florence, A. T. *Surfactant Systems*; Chapman and Hall: London, 1983.
(36) It is relevant to note that the Γ_{exc}^{max} values here for equivalent χ_s differ quantitatively from our previous calculation because the interface in our earlier work was defined as the plane at $Z' = X' + Y' - 1/2$. Thus the lowest energy conformation can have only $N/2 + 1$ monomers in direct contact with the interface, while all N monomers can lie in the $Z = 0$ plane in this paper.
(37) Private communication from Prof. E. Raphaël.
(38) The error bars are much larger for $N_b = 100$ and the bare surface than in Figure 5 because the larger attraction parameter (χ_s) reduces the quality of the statistics.

MA946043F